

Zhu Shouan (Orcid ID: 0000-0002-4973-1504)
Lotz Martin K. (Orcid ID: 0000-0002-6299-8799)

Running head: Excessive growth hormone promotes OA in mice

Excessive growth hormone promotes joint degeneration and chondrocyte metabolic dysfunction in mice

Shouan Zhu Ph.D.^{1,2*}, Huanhuan Liu Ph.D.^{1,2}, Trent Davis B.S.², Craig R.G. Willis Ph.D.^{1,2,8}, Reetobrata Basu Ph.D.³, Luke Witzigreuter B.S.⁵, Stephen Bell B.S.³, Nathaniel Szewczyk Ph.D.^{1,2}, Martin K. Lotz M.D.⁶, Marcheta Hill B.S.⁷, Roberto J. Fajardo Ph.D.⁷, Patrick M. O'Connor Ph.D.¹, Darlene E. Berryman Ph.D.^{1,3,4}, John J. Kopchick Ph.D.^{1,3,4*}

¹Department of Biomedical Sciences, Ohio University, OH, 45701, USA

²Ohio Musculoskeletal and Neurological Institute (OMNI), Ohio University, OH, 45701, USA

³Edison Biotechnology Institute, Ohio University, OH, 45701, USA

⁴Diabetes Institute, Ohio University, OH, 45701, USA

⁵Department of Biological Sciences, Ohio University, Athens, OH, 45701, USA

⁶Department of Molecular Medicine, The Scripps Research Institute, La Jolla, CA, 92037, USA

⁷School of Osteopathic Medicine, University of the Incarnate Word, San Antonio, TX, 78209, USA

⁸School of Chemistry and Biosciences, Faculty of Life Sciences, University of Bradford, Bradford, UK

*Correspondence to

Shouan Zhu: Department of Biomedical Sciences, Ohio Musculoskeletal and Neurological Institute (OMNI), Ohio University, OH, 45701, USA. zhus1@ohio.edu

John J. Kopchick: Department of Biomedical Sciences, Edison Biotechnology Institute, Diabetes Institute, Ohio University, OH, 45701, USA. kopchick@ohio.edu

This article has been accepted for publication and undergone full peer review but has not been through the copyediting, typesetting, pagination and proofreading process which may lead to differences between this version and the [Version of Record](#). Please cite this article as doi: [10.1002/art.42470](https://doi.org/10.1002/art.42470)

Conflict of interests: The authors have no conflicts of interest to declare.

Abstract

Objective: Many patients with acromegaly, a hormonal disorder with excessive growth hormone (GH), report pain in joints. The objective of this study is to characterize the joint pathology of mice with over-expression of either bovine GH (*bGH*) or a GH receptor antagonist (*GHa*). We also investigate the effect of GH on regulation of chondrocyte cellular metabolism.

Methods: Knee joints from mice over-expressing *bGH* or *GHa* and WT were histologically and μ CT analyzed for OA pathologies. Additionally, cartilage from *bGH* mice was used for metabolomics. Mouse primary chondrocytes from WT or *bGH* mice with or without Pegvisomant (Peg) treatment were used for Q-PCR and Seahorse Respirometry analysis.

Results: Both male and female *bGH* mice at ~13 months had increased knee joint degeneration, which is characterized by loss of cartilage structure, expansion of hypertrophic chondrocytes, synovitis, and subchondral plate thinning. The joint pathologies were also demonstrated by significantly higher OARSI and Mankin scores in *bGH* compared with WT mice. Metabolomics revealed changes of a wide range of metabolic pathways in *bGH* mice including beta-alanine metabolism, tryptophan metabolism, lysine degradation, and ascorbate and aldarate metabolism. Also, *bGH* chondrocytes upregulated fatty acid oxidation (FAO) and increased expression of *Col10a*. Joints of *GHa* mice are remarkably protected from developing age-associated joint degeneration with smooth articular joint surface.

Conclusions: These studies uncover that an excessive amount of GH promotes joint degeneration in mice, whereas antagonizing GH action through a *GHa* protects mice from OA development, which is associated with chondrocyte metabolic dysfunction and hypertrophic changes.

Introduction

Acromegaly is a hormonal disorder that most commonly occurs when a growth hormone (GH) secreting pituitary adenoma over-produces GH. If left untreated, joint pain and the associated mobility limitations are one of the most common clinical complications in patients with acromegaly. Either axial or peripheral arthropathy has been reported in more than 50% of these patients(1). Also, typical radiographic osteoarthritic changes, including joint space narrowing, osteophytosis, subchondral bony sclerosis, and cyst formation, can be identified in most of these patients(1, 2). Some argue that such pathological changes might not be indicative of an osteoarthritis (OA) diagnosis as these patients often also have radiographic signs in the hand and spine joints unlike those commonly seen in OA(3). Nevertheless, joint-associated pain is one of the most common complications that affect quality of life in patients with acromegaly(4, 5). By contrast, GH deficiency (GHD), if it occurs in children, can result in extremely limited skeletal growth and short stature, and is caused by insufficient amounts or lack of GH expression. One comparative study has found that the prevalence of radiographic OA is lower in elderly GHD patients than a normal population of elderly people(6). It is still unknown how GH disorders affect joint health over the lifespan.

Various animal models with altered GH levels or growth hormone receptor (GHR) dysfunction have provided insight into the functions of GH in joint health with mixed results. For example, studies examining hypopituitary dwarf mice (*dw/dw*) report that GH deficiency slows aging associated joint degeneration(7, 8). However, another study of dwarf rats (*dw/dw*) reported increased severity of articular cartilage lesions indicative of OA(9). By contrast, over-expression of bovine growth hormone (*bGH*) in mice increases cartilage clefts and synovial thickening at an early age of 6 months(10), suggesting increased GH action promotes OA development. Finally, a recent study using an inducible and isolated GH deficiency (AOiGHD) mouse line showed that adult-onset reduction of GH increases OA development(11). The different, and indeed, seemingly contradictory results from these studies are likely due to the use of different species and genetically modified animal lines within a given species. Thus, further investigations into the role of GH and the maintenance of joint health are needed.

Recently, emerging evidence demonstrated that impaired cellular metabolism in chondrocytes contributes to OA development(12). For example, decreased electron transport chain activity is found in OA chondrocytes and is associated with increased cartilage oxidative stress(13). Moreover, recent data demonstrate increased expression of various enzymes in the fatty acid oxidation (FAO) pathway in cartilage of mice on high fat diets(14, 15), implicating a possible linkage between a metabolic shift toward FAO in chondrocytes and obesity-induced OA development. Despite these important findings, it is still unknown how chondrocyte cellular metabolism is regulated during normal physiological conditions and dysregulated during OA.

GH is a strong regulator of central metabolism. During conditions of energy surplus, GH, in concert with IGF-1 and insulin, promotes nitrogen retention, and when food is sparse, GH increases use of lipids for conservation of vital protein and glycogen stores(16). GH is well-known for its role in promoting lipolysis(17). For example, baseline free fatty acids (FFA) values (~0.4 mmol/liter) usually more than double with peak values of approximately 1 mmol/liter recorded 2-3 hours after a single exogenous GH pulse in humans(17-21). In addition, *in vitro* bioassays based on the measurement of conversion of tritiated palmitate to $^3\text{H}_2\text{O}$ in human fibroblasts(18, 22) suggest that GH also directly stimulates FFA oxidation. No studies thus far have investigated the direct effects of GH on chondrocyte cellular metabolism and its implications in OA development.

The objectives of the current study were twofold: (1) to characterize OA development in mice with either over-expressed or suppressed GH action and (2) test if GH regulates chondrocyte function directly through altering chondrocyte cellular metabolism. We hypothesized that chronic GH overproduction leads to OA development via shifts in chondrocyte metabolism towards FAO. To test this hypothesis, we first characterize joint anatomy via both histopathology and micro-CT (μCT) from WT and *bGH* mice. We then used targeted liquid-chromatography mass spectrometry (LC-MS) to metabolically profile the cartilage tissue from these mice. In parallel and in an effort to better understand potential mechanisms by which GH regulates chondrocyte function, we isolated primary mouse chondrocytes from WT and *bGH* mice. These cells were then analyzed for expression of genes involved in chondrocyte hypertrophy, cartilage matrix synthesis and degradation. Additionally, we used Seahorse Respirometry to metabolically

characterize alterations of chondrocyte cellular metabolism with GH overexpression. Finally, we investigated whether mice over-expressing GHa are protected from developing OA.

Results

bGH mice develop increased knee joint degeneration at 13-months-old.

We first analyzed the joint histopathology of age-matched WT and *bGH* mice. At ~13 months of age, the articular cartilage of WT mice is largely intact with only undulating articular surface and mild loss of proteoglycan staining in the medial tibia (Figure 1A, upper panel). By contrast, the cartilage in *bGH* mice displayed multiple signs of moderate-to-severe degeneration. First, a large portion of non-calcified cartilage typically found in the medial femoral condyle is missing from the surface up to the tidemark (Figure 1A, lower panel, indicated by white arrowheads). This is consistent with the average OARSI and Mankin scores, which nearly doubled in *bGH* compared to WT mice (Figure 1B & 1C). Additionally, subcategory Mankin scores for articular cartilage structure and Safranin-O staining (Supplementary Figure 1A & 1B) are also significantly higher in *bGH* compared with WT mice. Second, multiple extrusions of cartilage tissue on both femoral and tibial articular surfaces can be seen (Figure 1A, lower panel, indicated by black arrowheads), indicating an early stage of osteophyte development. However, the osteophyte score is not significantly higher in the *bGH* relative to WT controls (Supplementary Figure 1A & 1B), this is likely be due to the fact that only osteophytes at the medial tibia were counted and included for the osteophyte score. Third, the tibial cartilage of *bGH* mice is hypercellular and consists of a large number of cells resembling hypertrophic chondrocytes in both calcified and non-calcified cartilage zones (Figure 1A, lower panel, indicated by black asterisks). Semi-quantification of the numbers of hypertrophic chondrocytes also showed approximately 90% increase in *bGH* mice (Supplementary Figure 1A & 1B), even though the number of tidemarks did not increase significantly (Supplementary Figure 1A & 1B). Interestingly, male and female mice have similar joint degeneration phenotype at this age (Figure 1B & 1C, Supplementary Figure 1A & 1B).

To assess if the joint degeneration is due to abnormal joint development in *bGH* mice, we analyzed the joints from age-matched WT and *bGH* mice at 3- and 6-months. Comparing with WT, *bGH* mice at 3 months develop normal joint structure with no signs of degeneration (Supplementary Figure 2A & 2B). By contrast, at joints in 6-month-old *bGH* mice exhibit early

Accepted Article

signs of OA with an uneven surface, loss of proteoglycan staining, and small lesions (Supplementary Figure 2C). This phenotype is also reflected by a significantly higher average Mankin score in *bGH* comparing with WT mice, though OARSI scores are not different between the two genotypes (Supplementary Figure 2D). Interestingly, this difference is only present in males but not females (Supplementary Figure 2D & 2E). These results suggest that the joint pathology in *bGH* mice develops during adulthood rather than being secondary to defective joint development. These results also suggest a potential sexual dimorphic effect of GH on OA disease development.

bGH mice develop synovitis and subchondral plate thinning.

Besides well-developed cartilage pathologies, synovium in *bGH* mice also exhibits hyperplasia. Compared with joints in WT mice, the synovial membrane in *bGH* mice was thickened, comprising 3-5 cell layers, and formed a subintimal stromal tissue adjacent to the joint capsule (Figure 1D). Interestingly, synovial hyperplasia was also apparent at the intercondylar notch (distal femur) and intercondylar eminence (proximal tibia) in the *bGH* mice (Figure 1D), indicating increased inflammation at the whole joint level. Consistently, grading for synovitis demonstrated a significantly higher score in both male and female *bGH* mice compared with WT controls (Figure 1E). Furthermore, subchondral bone in the tibia of *bGH* mice was visibly thinner than that in the WT mice as revealed in the Safranin O staining images (Figure 1F). μ CT results confirmed this observation (Figure 1G), with a relatively thin subchondral plate and lower BV/TV in *bGH* mice compared to WT control littermates (Figure 1H), indicating greater porosity in the subchondral bone of the *bGH* mice compared to the WT mice.

Chondrocytes in articular cartilage express functional GH receptor.

It has been demonstrated that chondrocytes in the growth plate express GH receptor (GHR)(23). To demonstrate if chondrocytes in the articular cartilage also express GHR, we immunohistochemically stained both mouse and human articular cartilage. To validate the result, we included joint tissue samples from mice with global GH receptor deficiency (*GHR*^{-/-}) (Figure 2A). It was found that both human and mouse cartilage abundantly express GHR (Figure 2A & 2B), while virtually no cells in the *GHR*^{-/-} are positively stained for GHR (Figure 2A). We didn't observe a difference of overall GHR expression level in normal vs OA cartilage tissue (Figure 2C). We then tested if chondrocytes in the articular cartilage would respond to GH treatment and

activate the canonical GH-induced intracellular signaling pathway: Janus kinase 2/signaling transducer and activator of transcription 5 (JAK-2/STAT-5). Acute bGH treatment of mouse primary chondrocytes increased tyrosine phosphorylated (Phos)-STAT5 in a dose-dependent manner (Figure 2D). The GHR antagonist, Peg, inhibited bGH induced activation of tyrosine Phos-STAT5 (Figure 2D & E). Consistently, immunofluorescent staining also showed significantly more chondrocytes expression of phos-STAT5 in *bGH* vs WT mice (Figure 2F & G).

Chondrocytes from bGH mice express higher levels of chondrocyte hypertrophy associated genes.

To further study the effect of GH on chondrocyte functions, we isolated chondrocytes directly from *bGH* mice and treated the cells with or without Peg. The cells were then used to examine the expression of genes associated with cartilage extracellular matrix, chondrocytes hypertrophy, and degradation of the cartilage matrix. Both aggrecan (*Acan*) and cartilage oligomeric matrix protein (*Comp*) expressions were significantly higher in *bGH* compared to WT chondrocytes, while type II collagen (*Col2a1*) did not change (Figure 3A, B, & C). Meanwhile, chondrocyte hypertrophy markers (type X collagen (*Col10a1*) and Adamts 5 but not *Mmp13*) were also significantly higher in *bGH* chondrocytes (Figure 3D, E, & F). Peg effectively decreased *Comp* expression to the basal level while it did not have a significant effect on other genes expression.

We also treated mouse primary chondrocytes with bGH alone or in combination with Peg for either a short (2 days) or a long (7 days) period of time. The cells were then used for gene expression analysis. Two days of bGH treatment significantly upregulated *Col2a1* and *Col10a1* expression (Supplementary Figure 4A & 4D) while it did not alter either *Acan* or *Comp* expression (Supplementary Figure 4B & 4C). Peg effectively normalized both *Col2a1* and *Col10a1* expressions to the basal levels (Supplementary Figure 4A & 4D). Similarly, two days of bGH treatment did not significantly affect either *Mmp13* or *Adamts 5* gene expression (Supplementary Figure 4E & 3F). Interestingly, prolonged bGH treatment (7 days) downregulated *Col2a1* expression by ~30% and *Acan* gene expression by nearly 50% (Supplementary Figure 5A & 5B). Peg failed to rescue the downregulation of *Col2a1* by bGH (Supplementary Figure 5A) but induced a significant recovery of *Acan* expression (Supplementary Figure 5B). Neither bGH alone nor bGH plus Peg significantly altered *Comp*

and *Coll10a1* gene expression (Supplementary Figure 5C & 5D) with 7 days treatment, suggesting a transient effect of bGH and Peg. Similar to the two-day treatment, neither bGH nor Peg treatment affected the gene expression of *Mmp13* and *Adamts 5* (Supplementary Figure 5E & 5F).

The intriguing higher level of chondrocyte hypertrophic gene *Coll10a1* expression in *bGH* chondrocytes prompted us to link to an interesting observation of the *bGH* mice joint histopathology that they have an increased number of large-size chondrocytes in both calcified and non-calcified cartilage zones (Figure 1A). In order to quantify this observation, we randomly quantified 10-15 chondrocytes from both calcified and non-calcified cartilage of each mouse and used Image J to measure cell sizes. Interestingly, in *bGH* males the average size of chondrocytes in the non-calcified cartilage but not the calcified is approximately 40% large than that in the WT controls (Figure 3G, upper panel & 3H). By contrast, *bGH* females exhibit significantly larger chondrocytes in both calcified and non-calcified cartilage relative to WT littermates (Figure 3I). In order to demonstrate if the enlarged cells are indeed hypertrophic chondrocytes, we used immunohistochemistry to stain joint sections for type X collagen (COLX). Interestingly, whereas the majority of stained chondrocytes are concentrated in the calcified cartilage in WT animals, COLX is robustly expressed throughout the full thickness of both calcified and non-calcified cartilage in the *bGH* mice (Figure 3G, lower panel).

Chronic GH over-production alters chondrocyte cellular metabolism.

Considering GH is a strong regulator of carbohydrate, lipid, and protein metabolism, we conducted a high-throughput targeted LC-MS analysis of small molecules (metabolites) to more broadly evaluate the role of GH in chondrocyte cellular metabolism. A total of 184 primary metabolites were detected and identified (see Methods section) in both WT and *bGH* cartilage samples. Principle Component Analysis (PCA) and Partial Least Squares-Discriminant Analysis (PLS-DA) plots of the results demonstrated a clear clustering of WT and *bGH* samples (Figure 4A). Forty-eight (48) metabolites were identified to have significantly different abundance values (Figure 4B). Interestingly, among them, only one metabolite, anserine, was downregulated while the other 47 metabolites were significantly upregulated in the *bGH* versus WT mice (Figure 4B). Anserine is a dipeptide comprised of a beta-alanine and a methylhistidine that has antioxidant activity under diabetic conditions(24). It is possible that GH may also

indirectly regulate oxidative stress through anserine metabolism in chondrocytes that further affect OA development. Analysis of variable importance projection (VIP) scores revealed 29 metabolites with VIP scores greater than 1 (Figure 4B). Pathway analysis of the important metabolites with *t*-test FDR < 0.1 and VIP score > 1 showed four pathways that are altered in *bGH* mice, namely: beta-alanine metabolism, tryptophan metabolism, lysine degradation, and ascorbate and aldarate metabolism. In order to identify potential interactions among the individual metabolites, we performed an interaction network(s) analysis for important metabolites using the Search Tool for Interactions of Chemicals (STITCH) database. Interestingly, we found that network hubs (i.e., nodes that have a high level of connectivity) included L-kynurenine, L-tryptophan, L-threonine, serotonin, L-lysine, homocitrulline, homo-L-arginine, and spermidine (Figure 4D). Also, the normalized concentrations of the two most connected metabolites, L-lysine and L-tryptophan are displayed as box plots in Figure 4E.

Chondrocytes from bGH mice have a higher basal fatty acid oxidation rate using palmitate as substrate.

Considering the strong effect of GH on fat metabolism, we further investigated how GH modulates fatty acid oxidation (FAO) in chondrocytes. Chondrocytes isolated directly from WT or *bGH* mice were used for Seahorse Respirometry assays (Supplementary Figure 8). During the assay, cells were provided BSA conjugated palmitate as substrate with sequential addition of medium or etomoxir (4 μ M), oligomycin (2 μ M), FCCP (1 μ M), and Rot/AA (0.5 μ M) to each well. *bGH* chondrocytes have a higher oxygen consumption rate (OCR) under the basal condition (Figure 5A & C). This is largely due to a higher FAO since the OCR of *bGH* chondrocytes dropped to a similar level of WT chondrocytes when FAO inhibitor Etomoxir was added (Figure 5A & D). Compared with WT, *bGH* chondrocytes also had a higher level of ATP-linked respiration (Figure 5G). No difference in non-mitochondrial respiration was observed between WT and *bGH* chondrocytes after treatment with the inhibitors Rot/AA (Figure 5B). Interestingly, *bGH* and WT chondrocytes had a similar maximal mitochondrial respiration after FCCP was injected (Figure 5E). Other parameters of mitochondrial function (e.g., proton leak, spare respiratory capacity, and coupling efficiency) did not differ between WT and *bGH* chondrocytes (Figure 5F, H, & I).

Mice over-expressing GH receptor antagonist are protected from developing OA.

To investigate if blocking GH action would protect mice from developing OA, we analyzed the knee joint of a dwarf mouse line expressing a *GHa*(25, 26) and its age-matched wild-type control (WT). At ~23 months of age, joints of WT mice exhibit early signs of aging-associated degeneration, characterized by an undulating articular joint surface and uneven intensity for proteoglycan staining (Figure 6A). In contrast, the articular joint surface of *GHa* mice was remarkably intact and smooth. The full thickness of cartilage in these mice was also evenly stained with proteoglycan. Both OARSI and Mankin grading systems were used to quantify the OA pathological changes. No significant difference of OARSI scores between WT and *GHa* was found (Figure 6B & C); however, the average Mankin score of *GHa* mice is significantly lower than that in the WT mice ($p = 0.0159$, Figure 6D). The difference is mainly attributed to lower subcategory scores for cartilage structure (Figure 6E) and Safranin-O staining (Figure 6G) in the *GHa* compared with the WT, while other parameters such as tidemark, osteophyte and hypertrophic chondrocytes are not different between WT vs *GHa*. These results suggest that over-expression of a functional GH receptor antagonist protects mice from developing aging associated OA joint degeneration.

Discussion

As the name implies, GH facilitates ‘growth’ by acting on the longitudinal bones; thus, to date almost all ‘bone’ studies have focused on the role of GH on chondrocyte proliferation in the growth plate cartilage during development. For example, studies in rat models demonstrated direct mitogenic effects of GH on growth plate chondrocytes(27, 28). The presence of GHRs, identified immunocytochemically using a monoclonal antibody to rabbit GHR, was demonstrated initially in the rabbit (23) and subsequently in the human (29) growth plate. These studies indicated the presence of direct GH targets in the growing mammal, with continued ontogeny of their distribution in the prepuberty period. More direct evidence found that after a single pulse of GH, tyrosine phosphorylated (p)-STAT5 was present in resting zone of the growth plate, and in particular, localized to the pre-hypertrophic chondrocytes(30). Despite the important role of GH in growth plate, little is known about the effect of GH on joint articular cartilage during growth or in cartilage maintenance, nor its implications for joint degeneration. For the first time, our study has found that chondrocytes in articular cartilage abundantly express GHR and initiate the canonical JAK/STAT5 signaling cascade upon GH stimulation. We further discovered that *bGH* mice developed increased articular cartilage degeneration and loss at ~13

months, with an increased number of hypertrophic chondrocytes. These results indicate that GH could possibly act directly on articular cartilage and promote chondrocyte pathological hypertrophic changes, further leading to cartilage degeneration. However, in order to delineate the role of GH on articular cartilage, the analysis of conditional GHR disrupted or knockout mice would be warranted in future studies.

Our study has demonstrated that GH may act directly on articular cartilage, though we could not rule out that some of the effects of GH on articular cartilage are indirectly influenced via IGF-1. It was originally thought that liver-derived insulin-like growth factor (IGF-1) is released into circulation and then mediates the effect of GH in the target tissues, a concept referred to as the somatomedin hypothesis(31). The somatomedin hypothesis was later revised as it was found that mice with liver-specific *Igf-1* gene knockout displayed normal postnatal body growth despite serum IGF-1 levels that were decreased by more than 80%(32). However, another study found that liver-specific GHR knockout mice which have 90% decrease of circulating IGF-1 were smaller than WT controls(33), suggesting IGF-1 is indeed important for normal body growth mediated by GH. Additionally, local treatment with GH to one leg, either through direct injection to the growth plate or as an infusion into the femoral artery, resulted in unilateral bone growth on the GH-treated side of hypophysectomized, GH-deficient rats(34). In one of our preliminary studies, we measured IGF-1 mRNA level locally in the cartilage tissue of WT vs *bGH* mice. There is indeed a higher level of IGF-1 expression with *bGH* overexpression (Supplementary Figure 3), suggesting a potential role of paracrine IGF-1 in the OA phenotype we observed in *bGH* mice. Given these findings, it is clear that additional investigations are necessary to dissect the relative contributions of endocrine and/or paracrine/autocrine levels of IGF-1 and GH to the development and maintenance of articular cartilage, and in particular, for any pathological changes manifesting during OA development.

Impaired cellular metabolism is a hallmark of aging and it is also a central feature of OA chondrocytes. For example, impaired electron transport chain activity in OA chondrocytes increases cartilage oxidative stress(13). In addition, significant aging associated decline in the activity of rate limiting glycolytic enzymes has also been reported(35), which could be linked to chondrocyte hypertrophic pathologic changes and OA development(36). Interestingly, GH secretion decreases during aging and a reduction in GH level is linked to healthy aging and

increased longevity. Indeed, the world's longest-lived laboratory mouse results from global disruption of the GH receptor gene (*GHR*^{-/-})(26), while *bGH* mice are short-lived with a maximal lifespan of only 18-months and a 1-year survival-rate of 25% (37, 38). In this study we completed a metabolomic profile and discovered that *bGH* overexpression led to alterations of different amino acid metabolic pathways, including those related to beta-alanine metabolism, tryptophan metabolism, lysine degradation, and ascorbate and aldarate metabolism. This is generally consistent with recent advances in metabolomics research showing differences in amino acid concentrations in the cartilage, synovial fluid, plasma, and urine of arthritic joints. For example, within equine cartilage explants, lysine was found to be elevated while alanine was decreased following TNF- α /IL-1 β treatment(39). Furthermore, increased abundance of metabolites in tryptophan metabolic pathway, such as tryptophan, kynurenic acid and anthranilic acid, have been found in the synovial fluid of patients with rheumatoid arthritis(40). Additionally, increased tryptophan metabolism has been found in the serum of rats with OA and has been suggested as a biomarker for OA(41). In the current study, we also used Seahorse Respirometry and for the first time discovered that GH promoted long-chain FAO in chondrocytes. Increased lipid metabolism in chondrocytes has been demonstrated to be linked to increased oxidative stress(42) and high-fat diet (HFD) induced OA development in mice(14). Considering the important roles of GH in lipid metabolism(17), it could be possible that GH also plays a role in the OA pathogenesis during HFD-induced obesity. Further studies to test if blocking FAO or GH signaling transduction inhibits chondrocyte metabolic dysfunction and OA development are needed.

Another novel finding from this study is that mice expressing functional GHa are protected from developing aging associated OA; this could potentially lay the foundation for future studies on testing the therapeutic potential of GHa for OA. Peg, an FDA approved drug to treat patients with acromegaly, was developed using the same *GHa* mouse model used in the current study(25). Following rigorous preclinical animal experiments(43) and human clinical trials in patients with acromegaly(44, 45), it was approved by FDA for treatment of these patients. We are not directly testing Peg *in vivo* in this study due to its relatively low activity in blocking GHR signaling in rodents(46). As demonstrated previously, glycine at positions 120 (G120) of human GH or position 119 of bovine GH is critical for its growth-promoting activity. Peg has nine amino acid changes including substitution of G120 with lysine (L) (G120L) as well as eight additional

changes that increase its ability to bind to the human GHR and not to the prolactin receptor. However, when used in rodents, Peg did not show effectiveness to block GH action(46), presumably due to the other 8 amino acid changes. In this study, we are taking advantage of a genetic mouse model with over-expression of bGH-G119R that has already been shown to effectively block GH actions in mice(25, 47). In fact, the resulting dwarf mice was the foundational data for the development of Peg. Our proof-of-concept studies will lay the foundation for future pharmacological design and production of a mouse specific GH receptor antagonist, which will be further tested in preclinical mouse models for OA treatment.

There are also several limitations of the study. First, we were not able to delineate the effect of body weigh/size of *bGH* and *GHa* mice on joint pathology and to dissect the cartilage specific role of GH-GHR signaling in the current study. We also noted the need for a larger sample size in our future studies. Additionally, OA pain associated behavioral tests will need to be included in our future studies to investigate the effects of GH on structural versus symptomatic OA pathologies. Last but not least, the use of bovine GH for transgene expression in mice versus mouse GH may result in a species-specific response in *bGH* mice, further effort to create a mouse model with overexpression of mouse GH would be warranted.

In conclusion, we reported an osteoarthritic phenotype in the knee joints of *bGH* mice and discovered chondrocytes with overactive GH actions had metabolic dysfunctions and pathological hypertrophic changes. Inhibition of GH actions through overexpression of a functional GH antagonist protected mice from developing aging associated OA. Future studies addressing cartilage specific functions of GH/GHR signaling in OA development and the translational potential of GH receptor antagonist, Peg, for OA treatment are warranted.

Methods

Additional detailed methods are provided in the supplemental materials.

Animals. Transgenic *bGH* (n=4 for male and n=5 for female) and *GHa* (G119R) (n=5, male) and WT controls (n=5 male and n=5 female for *bGH* mice control; n=4 male for *GHa* control) mice were group housed on corncob bedding with cardboard enrichment tubes and nestlets at $22 \pm 0.5^{\circ}\text{C}$ on a 14:10-hour light-dark cycle and maintained on a standard Chow diet until ~13 months of

age. The mice were euthanized with isoflurane in the fasted state (5-6 hours) and tissues were collected as described below. All animal procedures were reviewed and approved by the Institutional Animal Care and Use Committee at the Ohio University.

Acknowledgement

This work was supported by a research startup fund to SZ from Ohio University, a far/ANRF grant from Arthritis National Research Foundation to SZ (833836), and a FIRST award from the American Society for Bone and Mineral Research to SZ, an NIH grant R15AR080813 to SZ, a HF-AGE (AGE-008) grant from the Hevolution Foundation. a medical student seed grant from Ohio University to TD. We thank the Northwest Metabolomics Research Center and the University of Washington, Seattle supported by NIH S10 grant (1S10OD021562-01) for helping with the metabolomics analysis. JJK was supported by a grant by the State of Ohio's Eminent Scholar Program that includes a gift from Milton and Lawrence Goll and the AMVETS and JJK/DB by NIH grant R01AG059779. MKL was supported by a NIH Grant R37 AG059418. We thank Shane Profio and Austin Erdely for processing the 3- and 6-month-old WT/*bGH* mouse joints.

References

1. Layton MW, Fudman EJ, Barkan A, Braunstein EM, and Fox IH. Acromegalic arthropathy. Characteristics and response to therapy. *Arthritis Rheum.* 1988;31(8):1022-7.
2. Colao A, Pivonello R, Scarpa R, Vallone G, Ruosi C, and Lombardi G. The acromegalic arthropathy. *J Endocrinol Invest.* 2005;28(8 Suppl):24-31.
3. Tornero J, Castaneda S, Vidal J, and Herrero-Beaumont G. Differences between radiographic abnormalities of acromegalic arthropathy and those of osteoarthritis. *Arthritis Rheum.* 1990;33(3):455-6.
4. Kropf LL, Madeira M, Vieira Neto L, Gadelha MR, and de Farias ML. Functional evaluation of the joints in acromegalic patients and associated factors. *Clin Rheumatol.* 2013;32(7):991-8.
5. Miller A, Doll H, David J, and Wass J. Impact of musculoskeletal disease on quality of life in long-standing acromegaly. *Eur J Endocrinol.* 2008;158(5):587-93.

6. Bagge E, Eden S, Rosen T, and Bengtsson BA. The prevalence of radiographic osteoarthritis is low in elderly patients with growth hormone deficiency. *Acta Endocrinol (Copenh)*. 1993;129(4):296-300.
7. Silberberg R. Articular aging and osteoarthrosis in dwarf mice. *Pathol Microbiol (Basel)*. 1972;38(6):417-30.
8. Ewart D, Harper L, Gravely A, Miller RA, Carlson CS, and Loeser RF. Naturally occurring osteoarthritis in male mice with an extended lifespan. *Connect Tissue Res*. 2020;61(1):95-103.
9. Ekenstedt KJ, Sonntag WE, Loeser RF, Lindgren BR, and Carlson CS. Effects of chronic growth hormone and insulin-like growth factor 1 deficiency on osteoarthritis severity in rat knee joints. *Arthritis Rheum*. 2006;54(12):3850-8.
10. Vijayakumar A, Yakar S, and Leroith D. The intricate role of growth hormone in metabolism. *Front Endocrinol (Lausanne)*. 2011;2:32.
11. Poudel SB, Dixit M, Yildirim G, Cordoba-Chacon J, Gahete MD, Yuji I, et al. Sexual dimorphic impact of adult-onset somatopause on life span and age-induced osteoarthritis. *Aging Cell*. 2021;20(8):e13427.
12. Batushansky A, Zhu S, Komaravolu RK, South S, Mehta-D'souza P, and Griffin TM. Fundamentals of OA. An initiative of Osteoarthritis and Cartilage. Chapter 9: Obesity and metabolic factors in OA. *Osteoarthritis Cartilage*. 2021.
13. Mobasher A, Rayman MP, Gualillo O, Sellam J, van der Kraan P, and Fearon U. The role of metabolism in the pathogenesis of osteoarthritis. *Nat Rev Rheumatol*. 2017;13(5):302-11.
14. Donovan EL, Lopes EBP, Batushansky A, Kinter M, and Griffin TM. Independent effects of dietary fat and sucrose content on chondrocyte metabolism and osteoarthritis pathology in mice. *Dis Model Mech*. 2018;11(9).
15. Zhu S, Donovan EL, Makosa D, Mehta-D'souza P, Jopkiewicz A, Batushansky A, et al. Sirt3 Promotes Chondrogenesis, Chondrocyte Mitochondrial Respiration and the Development of High-Fat Diet-Induced Osteoarthritis in Mice. *J Bone Miner Res*. 2022.
16. Moller N, and Jorgensen JO. Effects of growth hormone on glucose, lipid, and protein metabolism in human subjects. *Endocr Rev*. 2009;30(2):152-77.

17. Kopchick JJ, Berryman DE, Puri V, Lee KY, and Jorgensen JOL. The effects of growth hormone on adipose tissue: old observations, new mechanisms. *Nat Rev Endocrinol*. 2020;16(3):135-46.
18. Djurhuus CB, Gravholt CH, Nielsen S, Pedersen SB, Moller N, and Schmitz O. Additive effects of cortisol and growth hormone on regional and systemic lipolysis in humans. *Am J Physiol Endocrinol Metab*. 2004;286(3):E488-94.
19. Gravholt CH, Schmitz O, Simonsen L, Bulow J, Christiansen JS, and Moller N. Effects of a physiological GH pulse on interstitial glycerol in abdominal and femoral adipose tissue. *Am J Physiol*. 1999;277(5):E848-54.
20. Krag MB, Gormsen LC, Guo Z, Christiansen JS, Jensen MD, Nielsen S, et al. Growth hormone-induced insulin resistance is associated with increased intramyocellular triglyceride content but unaltered VLDL-triglyceride kinetics. *Am J Physiol Endocrinol Metab*. 2007;292(3):E920-7.
21. Moller L, Dalman L, Norrelund H, Billestrup N, Frystyk J, Moller N, et al. Impact of fasting on growth hormone signaling and action in muscle and fat. *J Clin Endocrinol Metab*. 2009;94(3):965-72.
22. Cersosimo E, Danou F, Persson M, and Miles JM. Effects of pulsatile delivery of basal growth hormone on lipolysis in humans. *Am J Physiol*. 1996;271(1 Pt 1):E123-6.
23. Hill DJ, Riley SC, Bassett NS, and Waters MJ. Localization of the growth hormone receptor, identified by immunocytochemistry, in second trimester human fetal tissues and in placenta throughout gestation. *J Clin Endocrinol Metab*. 1992;75(2):646-50.
24. Peters V, Calabrese V, Forsberg E, Volk N, Fleming T, Baelde H, et al. Protective Actions of Anserine Under Diabetic Conditions. *Int J Mol Sci*. 2018;19(9).
25. Chen WY, White ME, Wagner TE, and Kopchick JJ. Functional antagonism between endogenous mouse growth hormone (GH) and a GH analog results in dwarf transgenic mice. *Endocrinology*. 1991;129(3):1402-8.
26. Coschigano KT, Holland AN, Riders ME, List EO, Flyvbjerg A, and Kopchick JJ. Deletion, but not antagonism, of the mouse growth hormone receptor results in severely decreased body weights, insulin, and insulin-like growth factor I levels and increased life span. *Endocrinology*. 2003;144(9):3799-810.

27. Oberbauer AM, and Peng R. Growth hormone and IGF-I stimulate cell function in distinct zones of the rat epiphyseal growth plate. *Connect Tissue Res.* 1995;31(3):189-95.
28. Guevara-Aguirre J, Balasubramanian P, Guevara-Aguirre M, Wei M, Madia F, Cheng CW, et al. Growth hormone receptor deficiency is associated with a major reduction in pro-aging signaling, cancer, and diabetes in humans. *Sci Transl Med.* 2011;3(70):70ra13.
29. Werther GA, Haynes K, Edmonson S, Oakes S, Buchanan CJ, Herington AC, et al. Identification of growth hormone receptors on human growth plate chondrocytes. *Acta Paediatr Suppl.* 1993;82 Suppl 391:50-3.
30. Gevers EF, Hannah MJ, Waters MJ, and Robinson IC. Regulation of rapid signal transducer and activator of transcription-5 phosphorylation in the resting cells of the growth plate and in the liver by growth hormone and feeding. *Endocrinology.* 2009;150(8):3627-36.
31. Daughaday WH, and Rotwein P. Insulin-like growth factors I and II. Peptide, messenger ribonucleic acid and gene structures, serum, and tissue concentrations. *Endocr Rev.* 1989;10(1):68-91.
32. Sjogren K, Liu JL, Blad K, Skrtic S, Vidal O, Wallenius V, et al. Liver-derived insulin-like growth factor I (IGF-I) is the principal source of IGF-I in blood but is not required for postnatal body growth in mice. *Proc Natl Acad Sci U S A.* 1999;96(12):7088-92.
33. List EO, Berryman DE, Funk K, Jara A, Kelder B, Wang F, et al. Liver-specific GH receptor gene-disrupted (LiGHRKO) mice have decreased endocrine IGF-I, increased local IGF-I, and altered body size, body composition, and adipokine profiles. *Endocrinology.* 2014;155(5):1793-805.
34. Isaksson OG, Jansson JO, and Gause IA. Growth hormone stimulates longitudinal bone growth directly. *Science.* 1982;216(4551):1237-9.
35. Nahir AM, Shomrat D, and Awad M. Differential decline of rabbit chondrocytic dehydrogenases with age. *Int J Exp Pathol.* 1995;76(2):97-101.
36. Nishida T, Kubota S, Aoyama E, and Takigawa M. Impaired glycolytic metabolism causes chondrocyte hypertrophy-like changes via promotion of phospho-Smad1/5/8 translocation into nucleus. *Osteoarthritis Cartilage.* 2013;21(5):700-9.
37. Bartke A. Can growth hormone (GH) accelerate aging? Evidence from GH-transgenic mice. *Neuroendocrinology.* 2003;78(4):210-6.

38. Junnila RK, List EO, Berryman DE, Murrey JW, and Kopchick JJ. The GH/IGF-1 axis in ageing and longevity. *Nat Rev Endocrinol.* 2013;9(6):366-76.
39. Anderson JR, Phelan MM, Foddy L, Clegg PD, and Peffers MJ. Ex Vivo Equine Cartilage Explant Osteoarthritis Model: A Metabolomics and Proteomics Study. *J Proteome Res.* 2020;19(9):3652-67.
40. Igari T, Tsuchizawa M, and Shimamura T. Alteration of tryptophan metabolism in the synovial fluid of patients with rheumatoid arthritis and osteoarthritis. *Tohoku J Exp Med.* 1987;153(2):79-86.
41. Zhao J, Liu M, Shi T, Gao M, Lv Y, Zhao Y, et al. Analysis of Serum Metabolomics in Rats with Osteoarthritis by Mass Spectrometry. *Molecules.* 2021;26(23).
42. Medina-Luna D, Santamaria-Olmedo MG, Zamudio-Cuevas Y, Martinez-Flores K, Fernandez-Torres J, Martinez-Nava GA, et al. Hyperlipidemic microenvironment conditionates damage mechanisms in human chondrocytes by oxidative stress. *Lipids Health Dis.* 2017;16(1):114.
43. Wilson ME. Insulin-like growth factor I (IGF-I) replacement during growth hormone receptor antagonism normalizes serum IGF-binding protein-3 and markers of bone formation in ovariectomized rhesus monkeys. *J Clin Endocrinol Metab.* 2000;85(4):1557-62.
44. Thorner MO, Strasburger CJ, Wu Z, Straume M, Bidlingmaier M, Pezzoli SS, et al. Growth hormone (GH) receptor blockade with a PEG-modified GH (B2036-PEG) lowers serum insulin-like growth factor-I but does not acutely stimulate serum GH. *J Clin Endocrinol Metab.* 1999;84(6):2098-103.
45. Trainer PJ, Drake WM, Katznelson L, Freda PU, Herman-Bonert V, van der Lely AJ, et al. Treatment of acromegaly with the growth hormone-receptor antagonist pegvisomant. *N Engl J Med.* 2000;342(16):1171-7.
46. Mode A, Tollet P, Wells T, Carmignac DF, Clark RG, Chen WY, et al. The human growth hormone (hGH) antagonist G120RhGH does not antagonize GH in the rat, but has paradoxical agonist activity, probably via the prolactin receptor. *Endocrinology.* 1996;137(2):447-54.

47. Chen WY, Wight DC, Wagner TE, and Kopchick JJ. Expression of a mutated bovine growth hormone gene suppresses growth of transgenic mice. *Proc Natl Acad Sci U S A*. 1990;87(13):5061-5.

Figure 1. *bGH* mice develop increased cartilage degeneration, synovitis, and subchondral plate thinning at 13-months-old. (A) Safranin O staining of knee joints of WT (upper panel) and *bGH* (bottom panel) mice. Low-magnification images (4x) of whole joints are on the left, high-magnification (20x) images of each joint compartments (lateral femur, medial femur, lateral tibia, medial tibia) are on the right. White arrowhead shows cartilage defects or loss, black arrowhead shows cartilage expansion and hypertrophy, * shows chondrocyte hypertrophic changes. Scale bar, 500 μm for 4x images, 100 μm for 20x images. (B-C) Quantification of OA severity in male (B) and female (C) WT and *bGH* mice using average (AVG) and maximal (Max) OARSI Scores, as well as average (AVG) Mankin Score that includes osteophyte, cartilage damage, tidemark duplication, proteoglycan Saf O staining, and hypertrophic chondrocytes. (D) Representative images of synovium from WT and *bGH* mice. Dashed black lines indicate areas of synovium hyperplasia. (E) Semi-quantitative synovitis scores in male and female WT and *bGH* mice. (F) Representative histological images of WT and *bGH* mice displaying thinning of the subchondral plate. Dashed white lines indicate areas of subchondral plate. (G) Representative images of μCT of tibial subchondral bone of WT and *bGH* mice. (H) Subchondral plate thickness (left graph) and percentage of bone volume to total volume (BV/TV) (right graph) of tibial subchondral bone of WT and *bGH* mice. * $p < 0.05$, ** $p < 0.01$, ns=not significant. n=5 for male WT, n=4 for male *bGH*, n=5 for female WT, n=5 for female *bGH* mice.

Figure 2. Chondrocytes in the articular cartilage tissue express functional GH receptor (GHR). (A) Immunohistochemical staining for GHR in lateral tibial cartilage of WT and GHR knockout (*GHR*^{-/-}) mice. Scale bar, 100 μm . n=3. (B) Immunohistochemical staining for GHR in human OA and normal articular cartilage. Scale bar, 100 μm . n=3 for Normal, n=4 for OA. (C) Ratio of GHR positively stained (GHR+) chondrocytes to total chondrocytes in Normal or OA human cartilage tissue. (D) Mouse primary chondrocytes were treated with 0, or 0.5 or 2.5 nM bGH with or without the GH receptor antagonist, Peg, and expression of phos-STAT5 (~95 kDa),

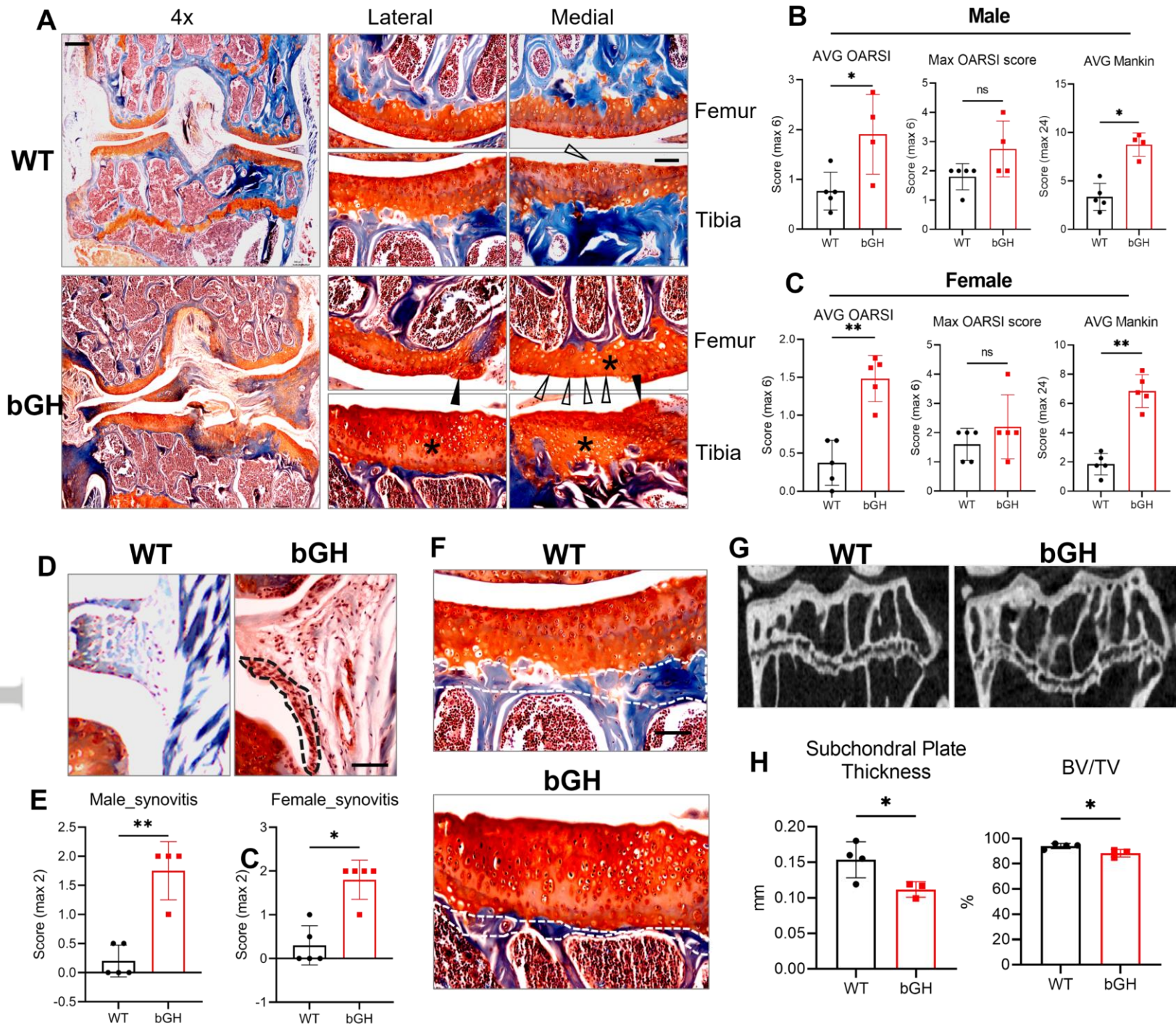
total STAT5 (Tot-STAT5) (~95 kDa), and beta-actin (ACTB) (45 kDa) was determined, n=5. (E) Densitometry analysis of ratio of phos-STAT5/total-STAT5 using blotting results from 5 independent experiments. (F) Immunofluorescent staining for phos-STAT5 in the cartilage of WT and *bGH* mice. (G) Ratio of phos-STAT5 positively stained (p-STAT5+) chondrocytes to total chondrocytes in WT and *bGH* mice cartilage. n=4, *p<0.05, scale bar, 100 μ m.

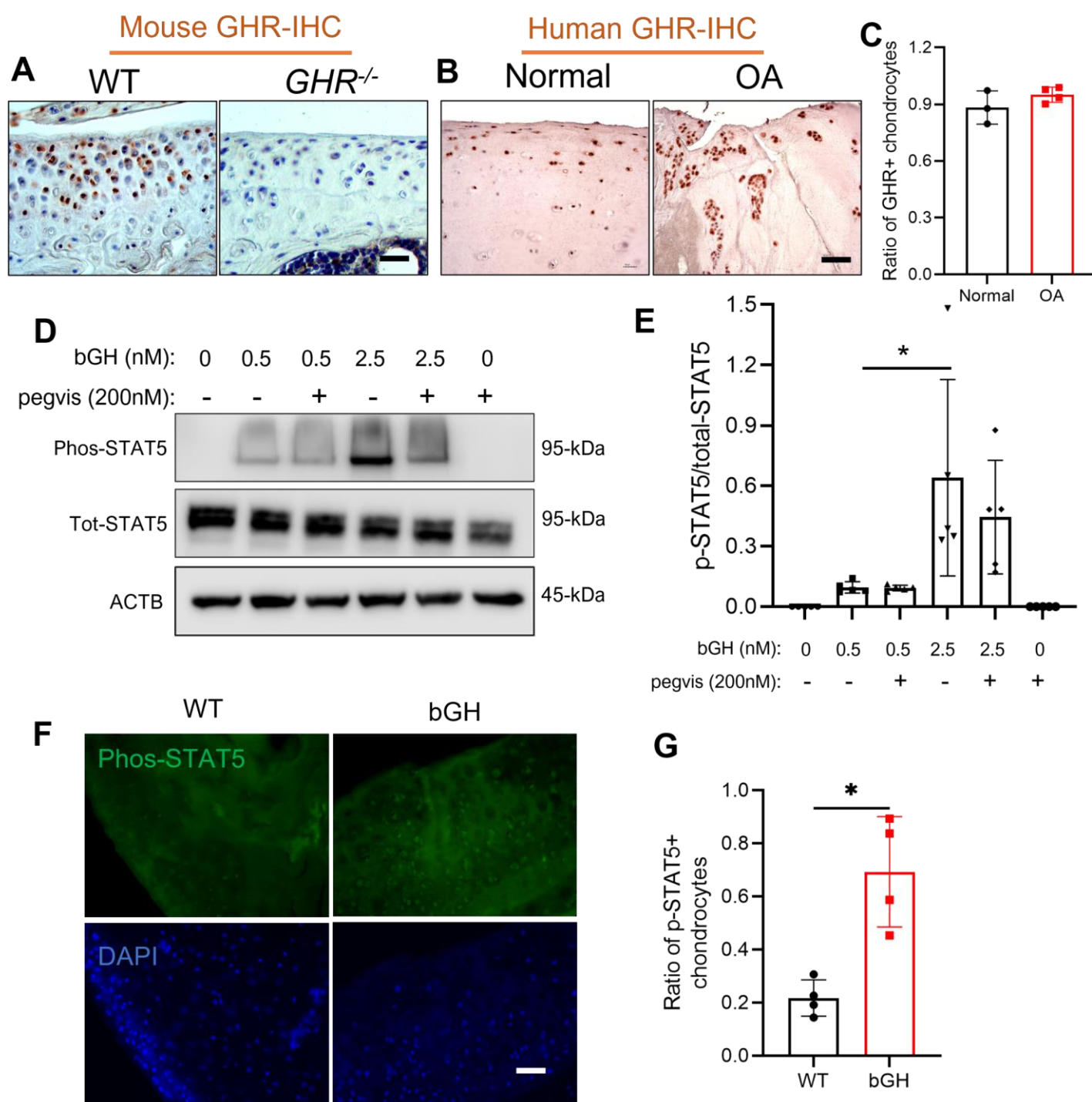
Figure 3. Chondrocytes from *bGH* mice express higher levels of chondrocyte hypertrophy associated genes. Mouse primary chondrocytes isolated from the articular cartilage of WT and *bGH* mice treated with or without Pegvisomant (200 nM) for two days were then used to detect gene expression of Col2a1 (A), aggrecan (Acan) (B), comp (C), Col10a1 (D), Mmp13 (E), and Adamts5 (F). *p<0.05, **p<0.01, ***p<0.001. n=3. (G) Safranin O staining and immunohistochemical staining for collagen type X (COLX) in the articular cartilage of WT and *bGH* mice. (H & I) Quantification of chondrocyte sizes in both non-calcified (n=75 for male WT, n=60 for male *bGH*, n=60 for female WT, n=75 for female *bGH*) and calcified (n=57 for male WT, n=48 for male *bGH*, n=40 for female WT, n=58 for female *bGH*) articular cartilage tissue in male (H) and female (I) mice. *p<0.05, ****p<0.0001, ns=not significant.

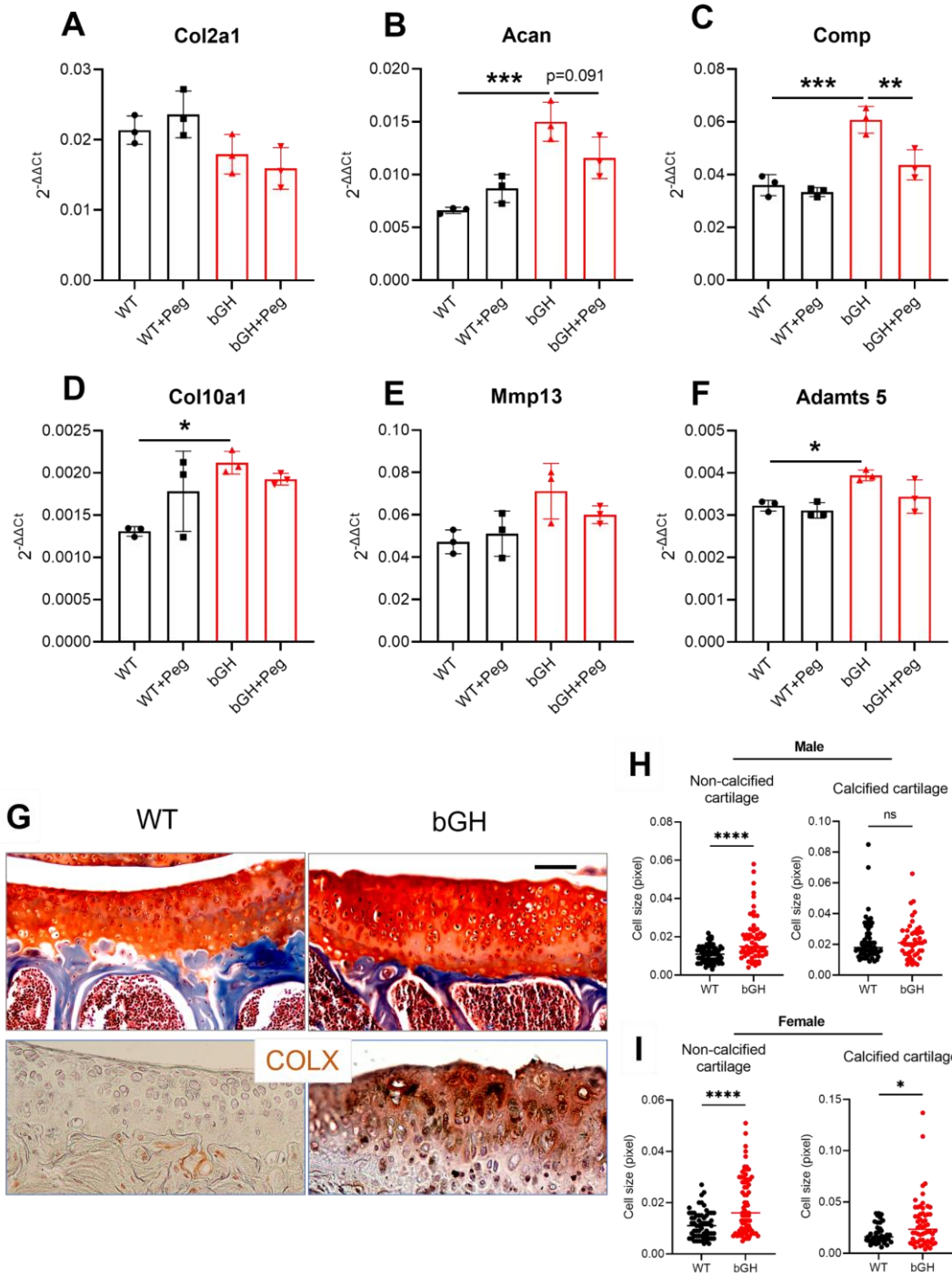
Figure 4: Metabolite analysis of *bGH* versus WT cartilage. Panel (A): PCA and PLS-DA plots showing extent of sample clustering per condition. Panel (B): Heatmap for metabolites with significantly different (*t*-test FDR < 0.1) concentrations in *bGH* versus WT samples. Also depicted is each feature's log₂ fold-change (LFC; with red and blue shading analogous with upregulation and downregulation in *bGH* samples, respectively) and PLS-DA derived variable importance projection (VIP) score. Panel (C): Pathway analysis of important metabolites (*t*-test FDR < 0.1 and VIP score > 1). Circle size is proportional to number of important metabolite 'hits' in given pathway, while strength of color shading is representative of -Log₁₀(*P*) for pathway enrichment (with darker shading analogous having stronger significance). Significantly enriched pathways are consequently labelled using in-plot. Panel (D): Interaction network(s) for important metabolites (*t*-test FDR < 0.1 and VIP score > 1), as defined using the Search Tool for Interactions of Chemicals (STITCH) database. Color shading is representative of LFC, red being upregulated and blue downregulated, in *bGH* samples (versus WT controls, respectively, with connecting edge thickness corresponding to strength of interaction. Panel (E): Box plots depicting normalized concentration for the two most connected metabolites in panel (D).

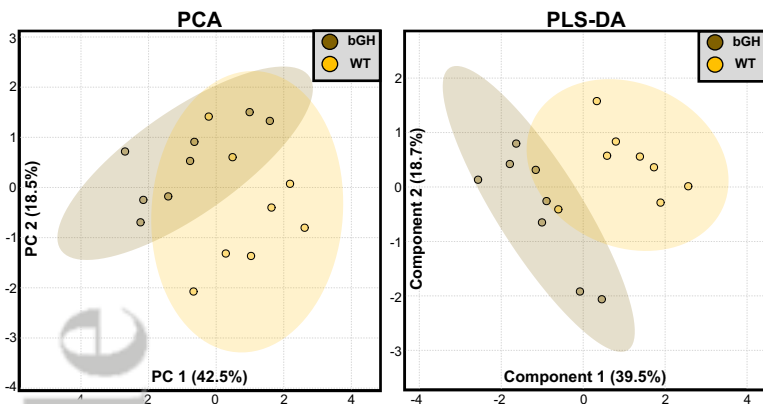
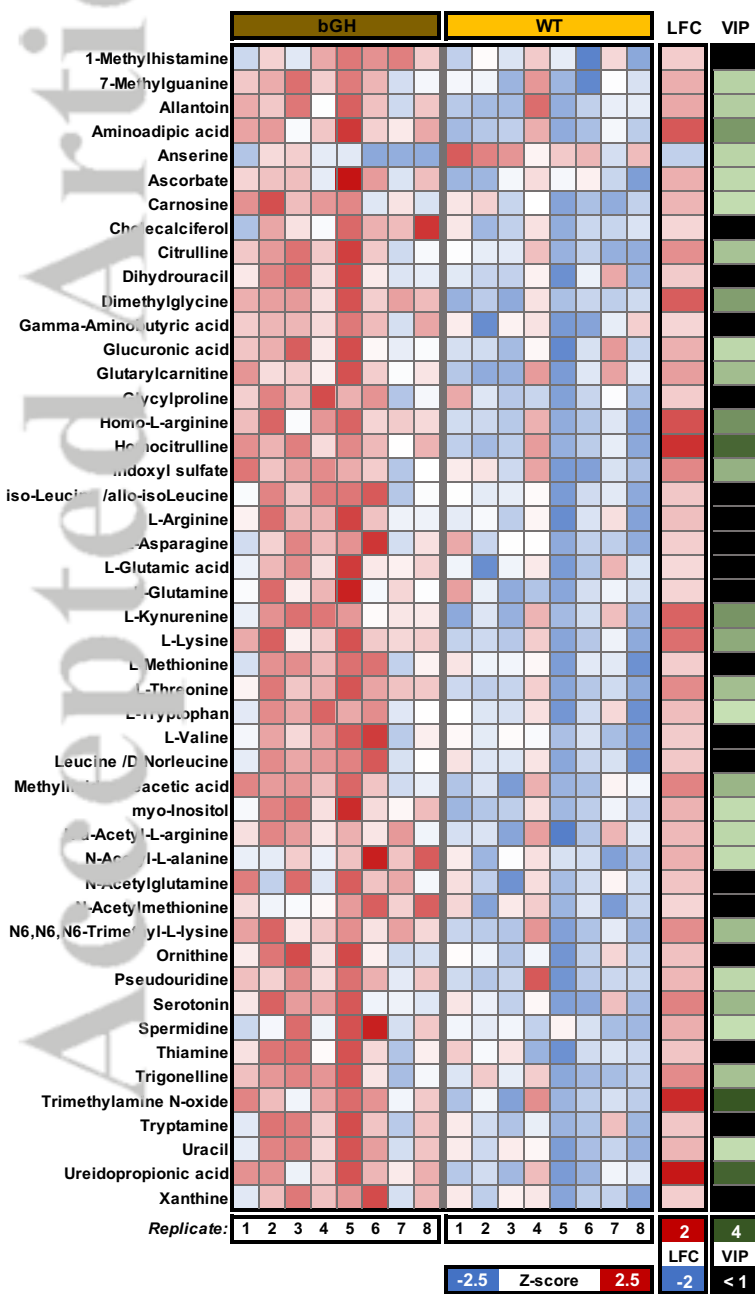
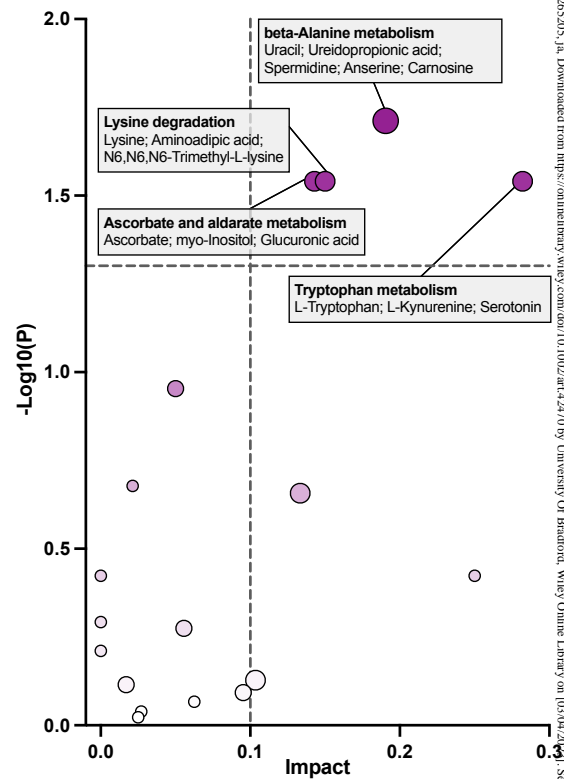
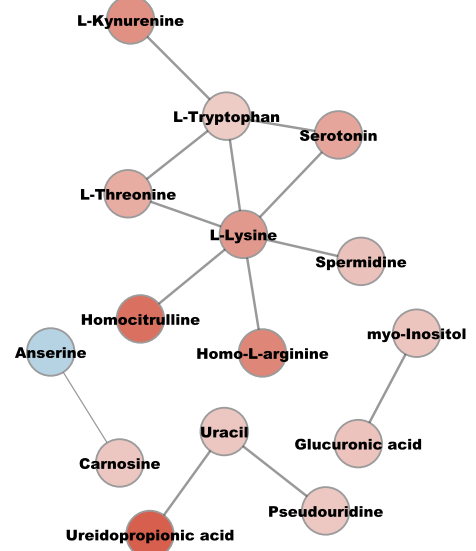
Figure 5. Chondrocytes from *bGH* mice are more efficient in oxidizing long-chain fatty acid palmitate using a Seahorse Respirometry assay. (A) Chondrocytes isolated from WT and *bGH* mice were provided BSA-conjugated palmitate as substrate. The cells were then subject to ‘Mito Stress Assay (acute injection)’ using Seahorse XFe24 analyzer. The first injection from Port A is either medium or the fatty acid oxidation inhibitor, Etomoxir (4 μ M), while the following three injections from Port B, C, D are: 2 μ M Oligomycin, 1 μ M FCCP, and 0.5 μ M Rotenone/Antimycin-A. Oxygen consumption rate (OCR, pmol/min/million cells) were measured during the assay. Data were then normalized to cell number. (B-I) Different aspects of mitochondrial functions including non-mitochondrial OCR (B), Basal Respiration_before extomoxir (C), Basal Respiration_after extomoxir (D), Maximal Respiration (E), Proton Leak (F), ATP Production linked Respiration (G), Spare Respiratory Capacity (H), and Coupling Efficiency (I) are calculated. * $p < 0.05$, **** $p < 0.0001$, $n = 4$.

Figure 6. Mice expressing a GH receptor antagonist (*GHa*) are protected from aging associated OA development. (A) Representative images of joints from ~23 months-old male WT and *GHa* mice. Upper panel, low-magnification images (4x). Lower panel, high-magnification images (20x) of the lateral tibia. Scale bar, 500 μ m for 4x images, 100 μ m for 20x images. Average (AVG) OARSI score (B), maximal (Max) OARSI score (C), average (AVG) Mankin score (D), cartilage structure (E), tidemark (F), Safranin O staining (G), oteophyte (H), hypertrophic chondrocyte (I) scores of WT and *GHa* mice joints. White arrowhead shows cartilage defects or loss, # shows loss of proteoglycan staining, * $p < 0.05$, ns=not significant. $n = 4$ for WT, $n = 5$ for *GHa*.







A**B****C****D****E**